Cone Penetration Tip Resistance Deconvolution Utilizing Complex Cepstrum Analysis

On June 22, 2018 Dr. Ross Boulanger gave a keynote lecture at the 4th International Symposium on Cone Penetration Testing (CPT'18) . The lecture was based upon the paper entitled "Inverse filtering procedure to correct cone penetration data for thin-layer and transition effects". This lecture and paper were of great interest to BCE as the technical objective was very similar to the challenging and highly published seismic deconvolution problem. BCE has invested considerable time and resource in developing algorithms for seismic deconvolution and seismic blind deconvolution. The unique characteristics of the described cone penetration convolution "blurring" function is highly suitable for implementation of Complex Cepstrum Analysis (CCA).

Cone Penetration Deconvolution Problem (after Boulanger and DeJong, 2018):

The measured cone penetration model, in general, is written as eq. (1)

$$q^m(z) = q^t(z) * w_c(z) + v(z) \quad (1)$$

where

$q^m(z)$: is the measured cone penetration.
$q^t(z)$: is the true cone penetration.
$w_c(z)$: is the "blurring" function.
$v(z)$: is additive noise, generally taken to be white with a Gaussian pdf.
$*$: denotes the convolution operation.

An alternative mathematical representation of $q^m(z)$ defined in eq. (1) is given as

$$q^m(z) = \int_{z_{min}}^{z_{max}} q^t(\tau) w_c(z-\tau) d\tau + v(z) \quad (2)$$

where z_{min} and z_{max} denote the limits of the CPT sounding.

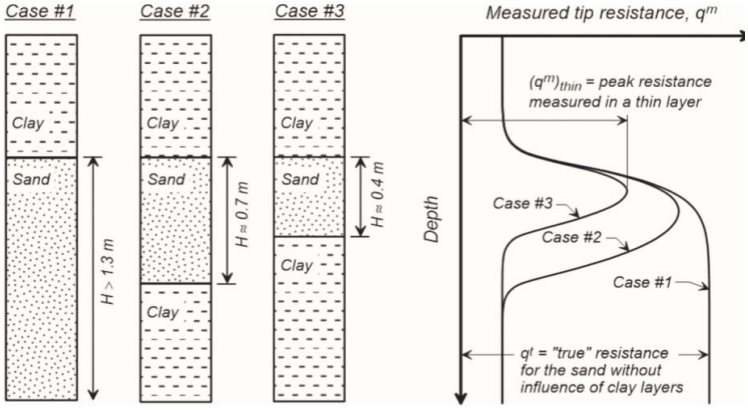

Figure 1. Schematic of thin layer effect for a sand layer embedded in a clay layer (after Boulanger and DeJong, 2018).

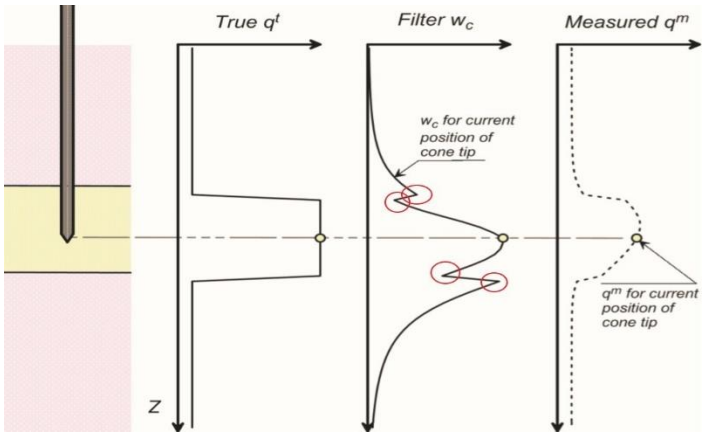

Figure 2. Illustration of the convolution of qt with the cone penetration "blurring" function to obtain q^m at a given point in a layered profile (modified from Boulanger and DeJong, 2018).

The discrete representation of eq. (2) is given

$$q^m(k) \;=\; \sum_{i=1}^{k} q^t(i) w_c\big(k-(i-1)\big) \;+ v(k), \quad k = 1,2 \cdots N \tag{3}$$

where N is the length of the depth series.

Figure 1 illustrates the effect the "blurring" function has on q^t. Figure 2 illustrates the convolution of w_c with q^t to give q^m at a given depth. Figure 2 clearly illustrates the typical form of w_c where the red circles identify sharp points at interfaces which require very high bandwidth frequencies. This w_c feature will be important within the application of CCA as will subsequently be outlined.

Boulanger and DeJong (2018) outline that w_c is depth variant and nonlinear in that it is dependent on q^t. Boulanger and DeJong (2018) utilize the following set of equations to iteratively obtain an estimate of q^t denoted as q^{inv}.

$$dq \;= q^t - q^m \tag{4}$$

$$dq \;= q^t - q^t * w_c(q^t) \tag{5}$$

$$q^t = q^m + dq \tag{6}$$

$$q^t = q^m + (q^t - q^t * w_c(q^t)) \tag{7}$$

$$q_{n+1}^{inv} = q^m + \big(q_n^{inv} - q_n^{inv} * w_c(q_n^{inv})\big) \tag{8}$$

$$err = \frac{\Sigma\left|(q_{n+1}^{inv} - q_{n+1}^{inv})_i\right|}{\Sigma|(q^m)_i|} =< \; 10^{-6} \tag{9}$$

Equation (7) is estimated iteratively by implementing eq. (8). In eq. (8), n denotes the n^{th} iteration and $q_1^{inv} = q^m$. The iteration process is continued until the error criterion defined by eq. (9) is met or a maximum number of user specified iterations is reached. Boulanger and DeJong (2018) state that the methodology defined by eq. (8) is not well constrained without additional adjustments. They believe that this is due to higher-than-justifiable spatial frequencies that are higher than justifiable based on the data sampling interval or physical size of the cone. A somewhat ad hoc smoothing filter followed by a low-pass spatial filter are applied to address this concern.

In general terms, it is surprising that iterative algorithm defined by eq. (8) has been shown to carry out the deconvolution process irrespective of the nonlinearity outlined by eq. (7). We believe this is most likely due to the case of $q^t \approx q^m$. This assumption is supported be the fact that $\boldsymbol{q_1^{inv} = q^m}$. The implementation of eq. (8) would not be possible for the case of seismic deconvolution where the reflection series is significantly different from the recorded seismogram. The purpose of this technical note is to outline a technique for obtaining an estimate of q^t without initializing $q_1^{inv} = q^m$ and based upon the high bandwidth of w_c.

Seismic Deconvolution Problem:

In seismology, the most important seismic model is, in general, written as

$$s(t) \;=\; b(t) * r(t) + \; v(t) \tag{10}$$

where

s(t): is the measured seismogram.
b(t) : is the seismic wave which is a superposition of earth and instrument responses.
r(t): is the reflectivity of the earth (reflection coefficients).
v(t): is the additive noise, generally taken to be white with a Gaussian pdf.
$*$: denotes the convolution operation.

The primary goal of seismic deconvolution is to remove the characteristics of the source wave from the recorded seismic time series, so that one is ideally left with only the reflection coefficients. The reflection coefficients identify and quantify the impedance mismatches between different geological layers that are of great interest to the geophysicist. This requires that the source wave is deconvolved from the seismogram. This goal is identical to that of estimating q^t (i.e., reflection series) by deconvolving w_c (i.e., source wave) from q^m (noisy seismogram). A very challenging and yet common seismic deconvolution problem is where the source wave is unknown and has the potential for time variation. This is referred to as blind seismic deconvolution (BSD) and identifies the case where we have one known (measured seismogram with additive noise) and two unknowns (source wave and reflection coefficients).

Seismic deconvolution is one of the most extensively study problem in geophysics with a vast amount of related publications. There are many techniques of seismic deconvolution that can be implemented so that an optimal estimate is made of the earth model. The majority of the standard seismic deconvolution methods utilize the steady state Wiener digital filter that assumes a minimum phase source wave. Other techniques implement inverse theory, minimum entropy deconvolution, adaptive deconvolution, principle phase decomposition, and Complex Cepstrum Analysis (CCA). Many of these deconvolution techniques are affected by the band-limited nature of the source wave. The one major advantage Cone Penetration Tip Resistance Deconvolution (CPTRD) is that the "blurring" function w_c has a high bandwidth signal as was illustrated in Fig. 2. This makes CCA a perfect candidate for incorporation into CPTRD.

Complex Cepstrum Analysis:

The governing equations defining CCA are summarized as below. Using the identity that the convolution operation in the time domain is a multiplication in the frequency domain and taking the frequency transform of eq. (10) (ignoring the noise term) gives

$$S(\omega) = B(\omega)R(\omega) \tag{11}$$

In eq. (11), S(ω), B(ω), and R(ω) are the Fourier transforms of *s(t)*, *b(t)*, and *r(t)*, respectively. Representing the Fourier transform of the processes in eq. (11) by their magnitudes and phases results in

$$|S(\omega)|e^{\gamma_S(\omega)i} = |BS(\omega)|e^{\gamma_B(\omega)i} \times |R(\omega)|e^{\gamma_R(\omega)i} \tag{12}$$

In eq. (12) γ(ω) is the phase of the process. Taking the Ln of both sides of eq. (12) and solving for R(ω) gives

$$Ln|R(\omega)| = Ln|S(\omega)| - Ln|B(\omega)| \tag{13a}$$
$$\gamma_R(\omega) = \gamma_S(\omega) - \gamma_B(\omega) \tag{13b}$$

the source wave (i.e., "blurring" function *b(t)*) and the noise free output seismogram (i.e., *s(t)* without measurement noise) allows us to deterministically determine the reflection series (i.e., *r(t)*). In CCA, eqs. (13a) and (13b) are applied on the recorded seismogram (*s(t)*) and known source wave (i.e., *b(t)*) to give the frequency spectrum of the reflection series (i.e., *R(ω)*). The inverse Fourier transform is then applied on *R(ω)* to give the desired reflection series (*r(t)*).

For example, Fig. 3(a) illustrates a simulated zero phase Klauder source wave (Vibroseis type source wave) which has a bandwidth of 4Hz to 140Hz as is shown in Fig. 3(b). The Klauder source wave is then convolved with the reflection series illustrated in Fig. 4(a) to give the output in Fig. 5(b). Applying eqs. 13(a) and 13(b) on the output shown in Figs. 3(a) and 5(a) and taking the inverse Fourier transform gives the results illustrated in Fig. 6. As is illustrated in Fig. 6, the reflection series is recovered exactly. Figure 7 illustrates the frequency ratio between seismogram and source wave.

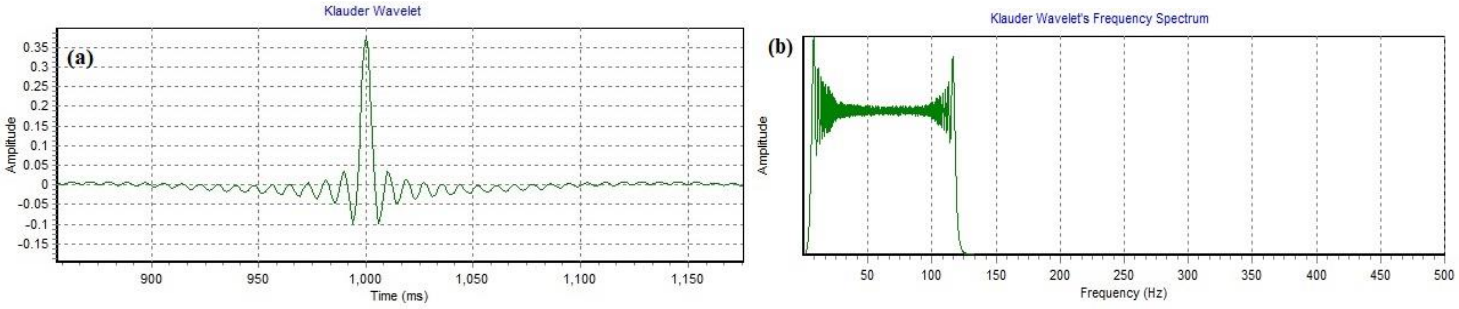

Figure 3. Simulation of the zero phase Klauder source wave (a) and corresponding frequency spectrum (b).

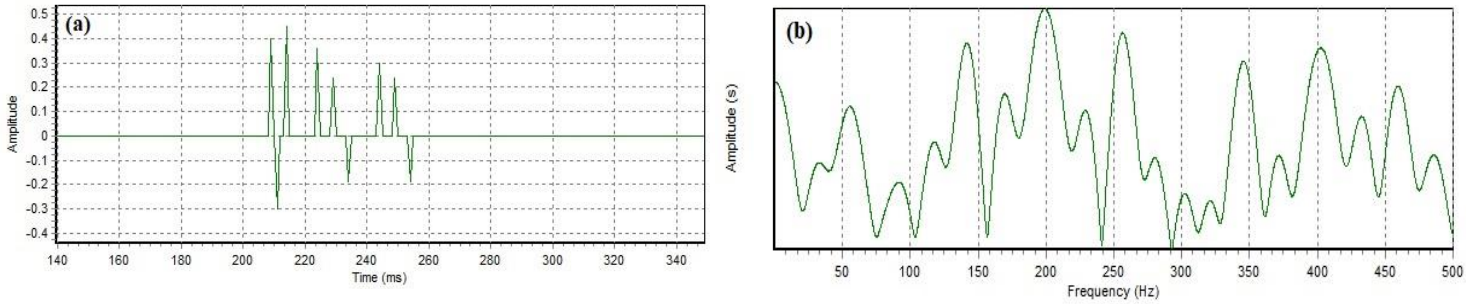

Figure 4. Reflection series (a) and corresponding frequency spectrum (b).

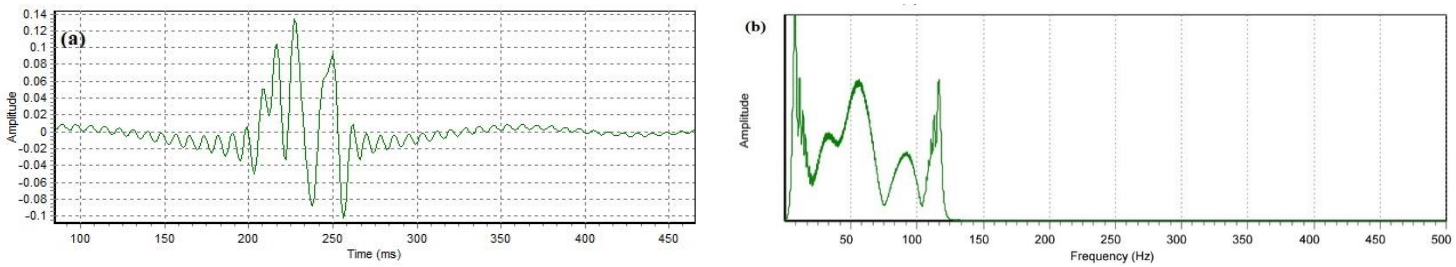

Figure 5. Simulated seismogram (a) and corresponding frequency spectrum (b).

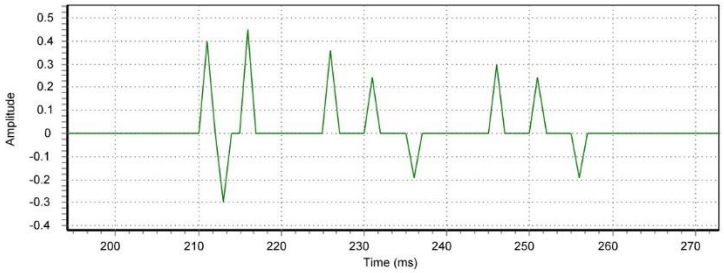

Figure 6. CSA estimated reflection series.

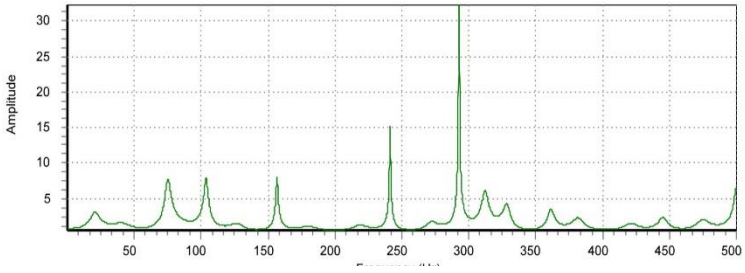

Figure 7. frequency spectrum ratio between source wave of Fig 3(a) and seismogram of Fig. 5(a).

The CCA works ideally in deconvolution if the seismogram is noise free. Equations (11) to 13 are updated below for the case measurement noise is considered. The error term in eq. (17) (i.e., $Ln\left|1 + V(\omega)/\left(S(\omega)R(\omega)\right)\right|$) can result in a dramatic degradation in the performance of CCA. The performance of CCA in the presence of measurement noise is directly dependent upon the frequency ratio of the source wave ("blurring" function) to the seismogram. The reflection series is a high bandwidth signal (see Fig. 4(b)); therefore, if the frequencies outside of the source wave's bandwidth (e.g., 4 Hz to 120 Hz (Fig. 3(b)) are negligible, then the CCA cannot estimate the reflection series *r(t)*. This is evident from the noise term ratio $V(\omega)/\left(B(\omega)R(\omega)\right)$ where $B(\omega) \rightarrow 0$ for frequencies outside its bandwidth and the noise term ratio becomes very large.

$$S(\omega) = B(\omega)R(\omega) + V(\omega) \tag{14}$$

$$S(\omega) = B(\omega)R(\omega)(1 + V(\omega)/B(\omega)R(\omega)) \tag{15}$$

$$Ln|Z(\omega)| = Ln|B(\omega)| + Ln|R(\omega)| + Ln\left|1 + V(\omega)/\left(B(\omega)R(\omega)\right)\right| \tag{16}$$

$$Ln|R(\omega)| = Ln|S(\omega)| - Ln|B(\omega)| - Ln\left|1 + V(\omega)/\left(B(\omega)R(\omega)\right)\right| \tag{17}$$

For example, Fig. 7 illustrates the Klauder source wave / seismogram frequency ratio for the case where no noise was present in the seismogram. As is shown in Fig. 7, there is measurable Klauder source wave to seismogram frequency information for all frequencies within the Nyquist. Fig. 8(a) illustrates the seismogram of Fig. 5(a) with measurement noise added. Figure 8(b) illustrates the frequency ratio of the source wave / seismogram for the output shown in Fig. 8(a).

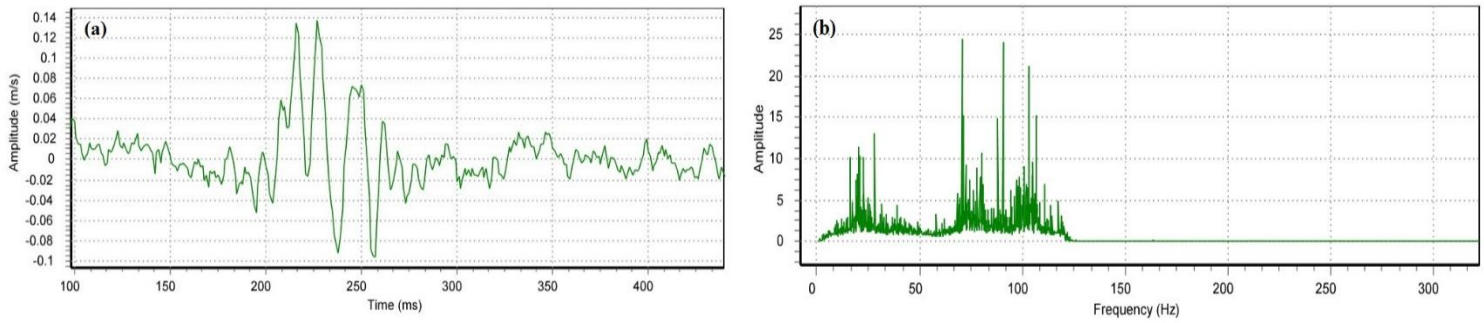

Figure 8. (a) Simulated seismogram of Fig 5(a) with measurement noise added. (b) Frequency spectrum ratio between source wave of Fig 3(a) and seismogram of Fig. 8(a).

As is shown in Fig. 8(b), frequency information above 120 Hz has almost been completely lost. This is due to the Klauder source wave having minimal signal information outside of the frequency band of 4 Hz to 120 Hz. Implementing CCA on the seismogram of Fig. 8(a) results in the nonsensical reflection series estimates illustrated in Fig. 10.

If the source wave had significant frequency information for frequencies ranging from 0 Hz to the Nyquist resulting in a broadband source wave / seismogram frequency ratio, then the CCA would produce desirable results. For example, consider the one-sided Klauder source wave illustrated in Figure 11(a). The sharpness of the peak response requires a

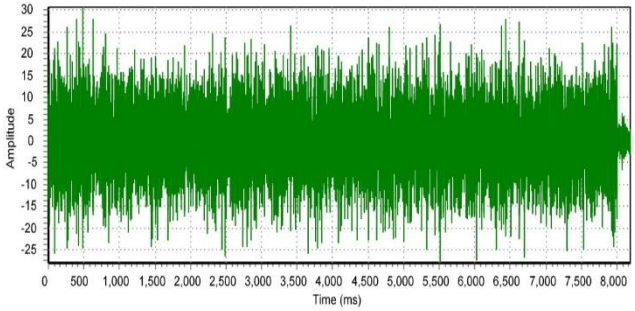

Figure 10. CSA estimated reflection series when measurement noise present.

large bandwidth of frequencies as is illustrated in Fig. 11(b). The resulting CCA estimate for this data set is illustrated in Fig. 12. Comparing Fig. 12 and 6, it is evident that there is very good agreement with the true reflection series.

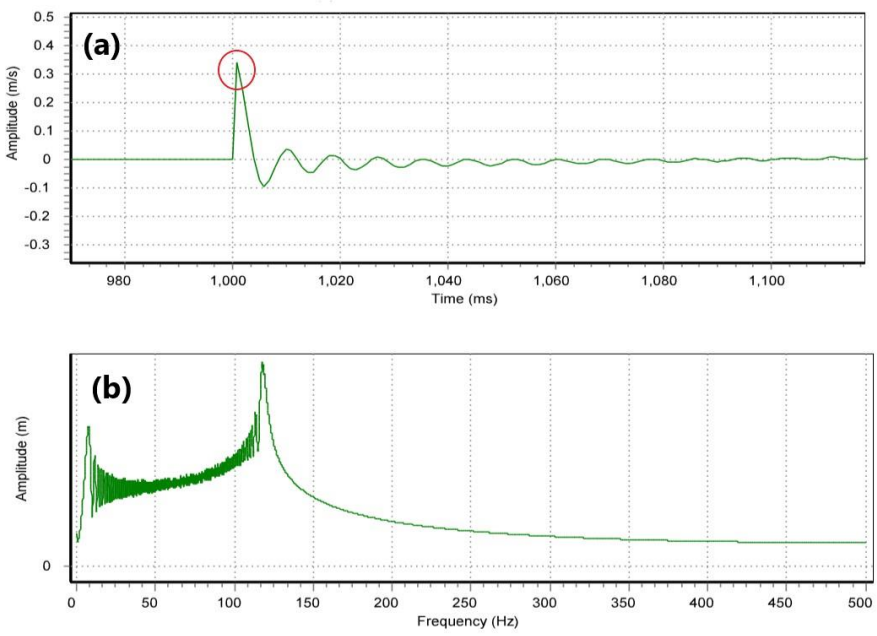

Figure 11. Simulation of the one-sided Klauder source wave (a) and corresponding frequency spectrum (b).

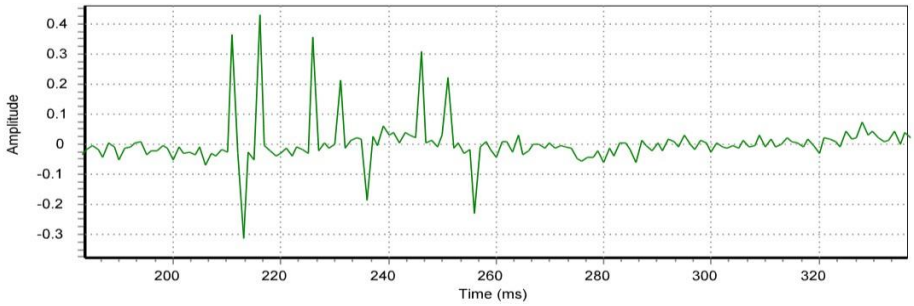

Figure 12. CSA estimated reflection series from seismogram generated with a one side Klauder source wave and the reflection series illustrated in Figs. 4 and 6.

Estimating q^t with CCA:

The form of the cone penetration "blurring" function w_c is ideally suited for CCA as was illustrated in Fig. 2. Figure 2 illustrated the typical form of w_c where the red circles identified sharp points at interfaces which require very high bandwidth frequencies.

The governing equations for CPT cone bearing deconvolution are nearly identical to that of seismic deconvolution where $q^m \rightarrow s(t)$, $w_c \rightarrow b(t)$, $r(t) \rightarrow q^t$, $Q^m(\omega) \rightarrow S(\omega)$, $W_c(\omega) \rightarrow B(\omega)$, and $R(\omega) \rightarrow Q^t(\omega)$. The proposed CCA algorithm for estimating q^t from q^m and $w_c(q^t)$ is outlined below where eq. (8) is updated to take into account a direct estimate of q^t when initializing the estimation iteration of eq. (8). In this case $q_1^{inv} = q^t(z)$ where is calculated using eqs. (18), (19) and (20). For the next subsequent iteration (i.e., $n = n+1$), $w_c(q^t, z)$ is calculated utilizing the previous estimate of q^{inv} (i.e., $w_c(z, q_{n-1}^{inv})$) and a new estimate of q_{n+1}^{inv} is obtained. This iteration process is continued until the error criterion defined by eq. (9) is met or a maximum number of user specified iterations is reached. It is also foreseen that a parameter estimation component could be incorporated into the CPTRD so that the w_c model parameters (e.g., m_z and m_q) could also be refined.

BCE will be shortly encoding an algorithm which incorporates the proposed CCA cone penetration tip resistance deconvolution algorithm. This technical note will subsequently be updated with results from a challenging test bed simulation.

$$q^m(z) = q^t(z) * w_c(z) + v(z) \quad (1)$$

$$err = \frac{\sum \left| \left(q_{n+1}^{inv} - q_{n+1}^{inv}\right)_i \right|}{\sum |(q^m)_i|} =< 10^{-6} \quad (9)$$

$$Q^m(\omega) = F(q^m) \quad (18a)$$

$$Q^t(\omega) = F(q^t) \quad (18b)$$

$$W_c(\omega) = F(w_c) \quad (18c)$$

where F denotes the Fourier transform

$$q^t(z) = F^{-1}\left(Q^t(\omega)\right) \quad (20)$$

where F^{-1} denotes the inverse Fourier transform

$$Ln|Q^t(\omega)| = Ln|Q^m(\omega)| - Ln|B(\omega)| \quad (19a)$$

$$\gamma_{Q^t}(\omega) = \gamma_{Q^m}(\omega) - \gamma_{w_c}(\omega) \quad (19b)$$

Erick Baziw
Gerald Verbeek